DMD Fast Forward. Published on June 13, 2007 as doi:10.1124/dmd.107.016493

DMD #16493

Title Page

Subcellular Trafficking Signals of Constitutive Androstane Receptor: Evidence for a Nuclear Export Signal in the DNA Binding Domain

Jun Xia[1], and Byron Kemper

Department of Cell and Development Biology (JX, BK) and Department of Molecular and Integrative Physiology (BK), University of Illinois at Urbana-Champaign, Urbana, IL, 60801

DMD Fast Forward. Published on June 13, 2007 as DOI: 10.1124/dmd.107.016493
This article has not been copyedited and formatted. The final version may differ from this version.

Running Title Page

Running Title: CAR trafficking signals

Corresponding author: Byron Kemper, Department of Molecular and Integrative Physiology, University of Illinois at Urbana-Champaign, 524 Burrill Hall, 407 S. Goodwin Ave. Urbana, IL 61801, Tel: 217-333-1146, Fax: 217-333-1133, Email: byronkem@uiuc.edu

Number of text pages:24

Number of tables: 0

Number of figures: 4

Number of references: 20

Number of words in Abstract: 245

Number of words in Introduction: 692

Number of words in Discussion: 1500

Abbreviations used are: CAR, constitutive androstane receptor; PB, phenobarbital; CCRP, CAR cytoplasmic retention protein; CRR, cytoplasmic retention region; LBD, ligand binding domain, glucocorticoid receptor interacting protein-1, GRIP1; NLS, nuclear localization signal, NES, nuclear import signal; SV40, simian virus 40; DBD, DNA binding domain; mCAR, mouse CAR; AF-2, activation function-2; XRS, xenobiotic response sequence; RNF, relative nuclear fluorescence

Abstract

Translocation of constitutive androstane receptor (CAR) from the cytoplasm to the nucleus is induced by phenobarbital-like drugs. Nuclear localization signals (NLS's) and a sequence (XRS) required for xenobiotic-induced nuclear translocation have been defined in rat and human CAR, but a nuclear export signal (NES) has not been identified. To identify cellular localization signals of CAR, the localization of fragments and mutants of mouse CAR expressed in mouse hepatocytes *in vivo* was examined. Consistent with other studies, an NLS in the hinge region, a diffuse NLS in the ligand binding domain, and a cytoplasmic retention sequence were identified, and mutation of the XRS blocked nuclear accumulation both in phenobarbital-treated mice *in vivo* and in untreated HepG2 cells. Fusing the simian virus 40 NLS to the mutant proteins, reversed the localization defect resulting from mutation of the hinge NLS but not that from mutation of the XRS indicating that the XRS is not simply a novel phenobarbital-responsive NLS. In the DNA binding domain, a sequence in CAR is conserved with an NES identified in other nuclear receptors. Mutation of two conserved phenylalanines in this sequence resulted in increased nuclear localization of both full-length CAR and a CAR fragment containing the DNA binding domain. The DNA binding domain sequence, therefore, may contain an NES, which is consistent with nucleocytoplasmic shuttling of CAR. The results demonstrate that regulation of the cellular localization of CAR is complex with multiple sequences mediating nuclear import and export and retention in the cytoplasm.

DMD Fast Forward. Published on June 13, 2007 as DOI: 10.1124/dmd.107.016493
This article has not been copyedited and formatted. The final version may differ from this version.

Constitutive androstane receptor (CAR) is an unusual nuclear receptor because of its constitutive activity (Baes et al., 1994) and its activation by phenobarbital (PB) without direct binding of PB to CAR (Moore et al., 2000; Tzameli et al., 2000). CAR is primarily a cytoplasmic protein in untreated animals in a complex with Hsp90 and CAR cytoplasmic retention protein (CCRP), a tetratricopeptide repeat protein, that interacts with the ligand binding domain (LBD) of CAR and retains CAR in the cytoplasm in cultured cells (Kobayashi et al., 2003; Yoshinari et al., 2003). After PB treatment, protein phosphatase 2A is recruited to the complex and CAR dissociates and translocates to the nucleus by an unknown mechanism. Retention in the cytoplasm prevents the chronic activation of target genes by the constitutively active CAR.

We have shown that exogenous expression of GRIP1 in mouse liver mediated nuclear accumulation of CAR without PB treatment and have proposed that CAR shuttles between the cytoplasm and nucleus in untreated animals and that activation of CAR by GRIP1 results in its nuclear retention and accumulation (Xia and Kemper, 2005). It has become increasingly clear that nuclear receptors dynamically shuttle between the nucleus and cytoplasm and that regulation of cellular localization is an important mechanism for regulating the activity of these nuclear receptors (Kawata, 2001; Maruvada et al., 2003). Nucleocytoplasmic shuttling of nuclear receptors requires specific nuclear localization signals (NLS's) (Kaffman and O'Shea, 1999) and nuclear export signals (NES's) (Fischer et al., 1995; Wen et al., 1995). Two NLS's and a cytoplasmic retention region have been identified in rat CAR (Kanno et al., 2005). A specific NLS, ^{99}LRRARQARRRA^{109} (critical residues underlined), in the hinge region was identified by mutational analysis. Deletion of the N-terminal 110 amino acids, including the hinge NLS, however, did not eliminate nuclear localization, and a second diffuse NLS was proposed within the sequence from amino acid residues 111 to 320. In addition to the NLS's, a cytoplasmic

retention region (CRR), which is a potential binding site for CCRP, was defined in the LBD by deletional analysis (Kanno et al., 2005).

Deletion of a leucine-rich peptide, LXXLXXL, in the LBD of human CAR, or mutation of the Leu residues, blocked nuclear translocation of the receptor after PB treatment (Zelko et al., 2001). This xenochemical response signal (XRS) is conserved in mouse and rat CAR and plays similar roles in their localization (Zelko et al., 2001; Kanno et al., 2005; Xia and Kemper, 2005). In cultured HepG2 cells, mouse CAR (mCAR) is predominantly nuclear, but mutation of the XRS results in cytoplasmic localization, and mutation of the XRS also blocks GRIP1-mediated nuclear translocation in untreated mice (Xia and Kemper, 2005). These results suggest that the XRS may be a PB-responsive NLS, but rat CAR fragments containing the XRS did not exhibit NLS activity (Kanno et al., 2005). Further, the XRS motif does not resemble a typical NLS signal, but is similar to leucine-rich protein interaction domains or, paradoxically, shares some sequence similarity with an NES found in the Ah receptor (Fischer et al., 1995; Wen et al., 1995; Ikuta et al., 1998). The XRS motif may, therefore, mediate the interaction with an unknown protein that results in nuclear accumulation of CAR (Zelko et al., 2001).

NES sequences have not been identified in CAR. Mutation of two Cys residues in the mCAR DBD resulted in a modest increase of nuclear localization of CAR in untreated animals suggesting that an NES might be present in the DBD (Xia and Kemper, 2005). A novel NES has been reported in the DBD's of other nuclear receptors (Black et al., 2001). The corresponding potential NES sequence in mCAR is ^{42}KGFFRRTV^{49}, and two highly conserved Phe residues (underlined) are critical for the NES function. To determine if CAR contains both NES and NLS sequences, we have examined by analysis of chimeras of GFP and mCAR mutants, potential subcellular localization signals of mCAR in cultured HepG2 cells and mouse hepatocytes *in vivo*.

The results provide strong evidence that an NES is present in the mCAR DBD, an NLS is present in the hinge region of mCAR, and that the XRS does not function simply as a PB-dependent NLS.

Materials and Methods

Plasmid constructions. The expression vector, pEGFPC1CAR, has been described (Min et al., 2002). Expression vectors for mutant mCAR in which Ala was substituted for Leu at positions, 322, 326, and 329, in the XRS, and in which the SV40 NLS was fused to either wild type mCAR or mutant mCAR with the three Ala substitutions in the XRS have been described (Xia and Kemper, 2005). The mutations in mCAR for the mutants, F44A/F45A**,** R107A/R108A, and 4RA(R100A/R101A/R107A/R108A), were introduced in pEGFPC1CAR by the QuikChange site-directed mutagenesis system as described by the manufacturer (Stratagene, La Jolla, CA). By the same method, the mutations F44A/F45A were introduced in CARDBD and the mutation R107A/R108A was introduced into NLSGFPCAR. For the deletion mutants, CAR(1–328), CARDBD (residues 18-86), CARHinge (residues 87-172), CARLBD (residues 173-358), and CAR(1-220), the sequences encoding the relevant amino acids were amplified by PCR and appropriate restriction digestion sites were introduced by the primers for insertion into pEGFPC1. To construct CAR(ΔCRR), the CAR sequences encoding 1-219 and 259-358 were amplified by PCR and appropriate restriction enzyme sites were introduced by the primers. The amplified fragments were digested with appropriate restriction enzymes, ligated together, and then inserted into pEGFPC1CAR.

Localization of chimeras of GFP and mCAR or the p160 coactivators in mouse hepatocytes *in vivo*. For *in vivo* transfections, plasmid DNA was isolated and injected into tail veins of six to eight week-old (20–25 g) BALB/c male mice (Harlan Labs) using the TransIT In Vivo Gene Delivery System (Mirus Bio Corp.) as described (Xia and Kemper, 2005). Two hr after injection of the DNA, the mice were injected intraperitoneally with either isotonic saline or 100 μg/g body weight of PB, and after an additional 4 hr, the mice were sacrificed. The livers were cut into

small pieces, placed in Tissue-Tek O.C.T. Compound (Miles, Inc.), and frozen in liquid N_2. Frozen sections of 10 µm were prepared with a cyrostatic microtome. Fixation, staining of nuclear DNA with propidium iodide, and detection of fluorescence were performed as described (Min et al., 2002). The average intensity of fluorescence in the nucleus and cytoplasm was determined using ImageJ software to measure the average intensity in the whole cell and the nuclear compartment. Relative nuclear fluorescence (RNF) was calculated by dividing the average intensity of fluorescence in the nucleus by the average intensities in the whole cell (nucleus + cytoplasm) as before (Min et al., 2002). At least 40 cells from at least two mice were randomly selected for analysis for each GFP construction. Statistical differences between the means of the RNF values of two groups were tested by the Student's t-test with an assumption of unequal variances.

Results

Localization of mouse CAR fragments containing the hinge domain or the LBD. To determine whether NLS sequences were present in mCAR, fragments of mCAR were fused to GFP (Fig. 1) and the cellular localizations of the chimeric proteins were determined in hepatocytes transfected *in vivo*. Representative images of cells that fall into each of the four categories of RNF, <0.25, 0.25-0.5, 0.5-0.75, and >0.75 are shown in Figure 2. Staining with propidium iodide marks the nucleus and the intensity of GFP fluorescence in the nucleus and whole cell was determined to calculate the RNF, the ratio of the green fluorescence intensity in the nucleus compared to that in the whole cell.

NLS's have been identified in the hinge and LBD domains of rat CAR based on experiments in cultured rat RL34 cells (Kanno et al., 2005), and mutation of the hinge motif blocked PB-induced nuclear translocation in rat primary hepatocytes. To determine whether these NLS activities were present in mCAR and functioned *in vivo*, hepatocytes of untreated or PB-treated mice were transfected with the expression vector of GFPCARHinge or GFPCARLBD by tail vein injection of plasmid DNA. In untreated animals, GFPCARHinge was predominantly cytoplasmic, similar to full length wild type mCAR (Fig. 3A, a, b). After PB treatment, the percentage of the cells examined that exhibited primary nuclear localization (RNF>0.5), increased from 5% to 22%, with the mean RNF significantly different from the untreated sample, but the increase was significantly less than the increased nuclear accumulation of wild type mCAR after PB treatment. Similarly, GFPCARLBD is primarily localized in the cytoplasm in the absence of PB (Fig 3A, c). After PB treatment, a shift to the nucleus was observed and the cells with primary nuclear localization (RNF>0.5) increased from 2% to 35% again a significantly smaller shift than observed with wild type mCAR (Fig 3A, a). These results

indicate that both the hinge domain and the LBD retain partial NLS activity after PB treatment, but neither of the two domains alone is sufficient for maximal nuclear import of mCAR.

The XRS motif is not simply an NLS. The function of the XRS motif remains unclear. It is required for nuclear translocation after PB treatment (Zelko et al., 2001; Xia and Kemper, 2005), for nuclear accumulation in untreated cultured cells (Xia and Kemper, 2005), and for GRIP1-mediated nuclear translocation *in vivo* in untreated mice (Xia and Kemper, 2005). In cultured cells, fusion of an NLS sequence to mCAR mutated in the XRS, partially restores nuclear accumulation suggesting the XRS is functioning as an NLS in these cells (Xia and Kemper, 2005). On the other hand, rat CAR XRS fragments did not exhibit NLS activity in cultured cells (Kanno et al., 2005). If the XRS motif functions as an NLS that is masked by some mechanism or blocked by a cytoplasmic retention signal in untreated animals but becomes functional after PB treatment, then fusion of a strong NLS to CAR mutated in the XRS should restore nuclear accumulation after PB treatment *in vivo*. As shown previously (Xia and Kemper, 2005), mutation of three Leu residues in the XRS has little effect on cellular distribution of mCAR in untreated animals, but prevents nuclear localization after PB treatment (Fig. 3B, a). Fusion of the SV40 NLS sequence to wild type GFPCAR resulted in a moderate statistically significant shift of mCAR to the nucleus in untreated mice with an increase from 5% to 40% of cells with mCAR predominantly in the nucleus (Fig 3B, b). A similar shift to nuclear localization in untreated mice was observed for NLSGFPCARL322/6/9A (Fig. 3B, c), providing evidence that the fused NLS was functional. PB treatment resulted in modest, but statistically significant, additional nuclear localization of wild type NLSGFPCAR(Fig. 3B, b) so that the final distribution was similar to that of wild type GFPCAR (Fig. 3A, a) after PB treatment. In contrast, PB treatment did not increase the nuclear localization of NLSGFPCARL322/6/9A (Fig. 3B, c), consistent with

the lack of nuclear translocation of GFPCARL322/6/9A after PB treatment. These results are not consistent with the XRS functioning solely as an NLS after activation by PB since if this were the case, mutation of the XRS should not inhibit PB-mediated nuclear translocation if a strong NLS is present.

^{99}LRRARQARRRA^{109} in the mCAR hinge domain is an NLS signal. The sequence ^{99}LRRARQARRRA^{109} located in the hinge domain of rat CAR was reported to be an NLS signal (Kanno et al., 2005) and is highly conserved in mCAR. Arg residues critical for the NLS function are underlined. Deletion of the hinge domain, however, did not prevent nuclear translocation of human CAR (Sueyoshi et al., 1999) suggesting that the NLS sequence in the hinge region was not functionally important. To examine the function of this sequence in mCAR after PB treatment, Ala was substituted either for Arg-107 and Arg-108 or for all of the critical Arg residues in the NLS analogous to the mutations made in rat CAR. These two mutants were then transfected into mouse hepatocytes *in vivo* by tail vein injection and the mice were treated with PB. Compared to wild type mCAR, the percentage of cells expressing the R107A/R108A mutant for which fluorescence was primarily nuclear (RNF>0.5) decreased from 63% to 30% and the RNF mean value was significantly less than that of wild type (Fig. 3C, a). Similar results were obtained if all four Arg residues were mutated (Fig. 3C, b). These results are consistent with previous studies of rat CAR (Kanno et al., 2005). Interestingly, for the fraction of cells in which the mutant protein was primarily nuclear, nearly all were strongly nuclear (RNF>0.75). These data suggest that factors other than the hinge NLS predominately mediate nuclear localization in a subset of cells.

If the hinge sequence is functioning as an NLS, then fusion of an NLS to the hinge mutants should restore the nuclear localization of mCAR. As shown in Fig. 3C, c, fusion of the

SV40 NLS to R107A/R108ACAR resulted in nuclear accumulation of fluorescence in untreated mice similar to that of wild type mCAR fused to the NLS (Fig. 3C, c and Fig 3B, b). After PB treatment, a modest, but statistically significant, additional nuclear accumulation of R107A/R108ACAR was observed similar to that observed for wild type NLS-mCAR. This contrasts with the impaired nuclear accumulation of R107A/R108ACAR (Fig. 3C, a) compared to wild type (Fig. 3A, a) after PB treatment. The fused NLS, therefore, compensates for the mutations in the hinge region which is consistent with an NLS function for this region.

Loss of cytoplasmic retention is not sufficient for maximal nuclear import of mouse CAR. In rat CAR, a cytoplasmic retention signal (CRR) was identified within the sequence from residue 220 to 258 (Kanno et al., 2005). To investigate the function of the CRR region in mCAR in hepatocytes *in vivo*, we constructed GFP chimeras of mCAR fragments truncated to residue 220, CAR(1-220) or with residues 200-258 deleted, CAR(ΔCRR) analogous to the rat CAR mutants that were analyzed. In untreated animals, primary nuclear localization of fluorescence was observed in 34% and 21% of cells for CAR(1-220) and CAR(ΔCRR), respectively, compared to only 5% for wild type mCAR and the RNF mean values were significantly increased (Fig 3D, a and b). These results are qualitatively similar to the rat studies, although in rat studies the mutant CARs were predominantly nuclear in 79% of cells. The results are consistent with a cytoplasmic retention function for the 220-258 region.

The effect of PB treatment on the localization of CAR(ΔCRR) was examined since this construction retains the XRS and should be responsive to PB. However, there was no statistically significant difference in the nuclear localization of CAR(ΔCRR) after PB treatment (Fig 3D, b). These data suggest that deletion of the CRR region not only results in a shift to the nucleus in untreated mice, but also substantially reduces PB-mediated nuclear import.

Does the CAR DBD contain an NES? The PB-independent nuclear translocation of mCAR in mouse hepatocytes *in vivo* mediated by exogenous expression of GRIP1 in untreated animals led to a proposal that CAR was shuttling between the nucleus and cytoplasm (Xia and Kemper, 2005). Further, mutation of two Cys in the CAR DBD resulted in modest nuclear accumulation of mCAR *in vivo*. A conserved sequence, containing two critical Phe residues, in the DBD of several steroid and orphan nuclear receptors has been reported to be critical for receptor nuclear export (Black et al., 2001). To determine if an NES was present in the mCAR DBD, Ala was substituted for the critical Phe residues 44 and 45 in full length or a truncated mutant, CARDBD (amino acids 18-86), that contains the DBD. In untreated animals, a substantial statistically significant shift to the nucleus was observed for the F44/F45A mutant with about 40% of the cells predominantly nuclear compared to 5% for wild type (Fig. 4A, B). The truncated CARDBD remained primarily cytoplasmic (RNF<0.5), but contained more cells with predominantly nuclear localization than the full length wild type mCAR (Fig. 4C). Since the hinge region NLS, the CRR motif and the XRS motif are all deleted in CARDBD, translocation into the nucleus presumably represents passive diffusion of the relatively small GFPCARDBD (MW ~35 kDa) into the nucleus, in contrast to the larger full length GFPCAR (MW ~68 kDa), which is also bound to other proteins in the cytoplasm (Yoshinari et al., 2003). Mutation of the two Phe in the CAR DBD fragment resulted in a significant additional shift to the nucleus with the percentage of cells primarily nuclear (RNF>0.5) increasing from 35% (Fig. 4C) to 87% (Fig. 4D). The substantial shift from the nucleus to the cytoplasm for both the full length mCAR and the CARDBD when the two Phe critical for NES function in other nuclear receptors are mutated strongly indicates that the CAR DBD has an NES function *in vivo*.

Discussion

Our previous study on the GRIP1-mediated nuclear accumulation of mCAR led us to propose that GRIP1 mediates the PB-independent nuclear accumulation of mCAR by activating and retaining mCAR in the nucleus (Xia and Kemper, 2005). This suggests that even in untreated animals, mCAR is not simply sequestered in the cytoplasm but constantly shuttles between the nucleus and cytoplasm and implies that mCAR contains both NLS's and NES's. In the present work, nuclear import activity was found to be present in the hinge domain and the LBD of mCAR. These results from *in vivo* studies are consistent with the cell culture studies of rat CAR in which an NLS was identified in the hinge domain and a second NLS-like activity diffusely within the LBD (Kanno et al., 2005). The rat CAR hinge NLS is conserved in mCAR and mutation of this sequence in mCAR partially blocked PB-induced nuclear accumulation confirming that the mouse sequence has NLS activity. Decreased PB-induced nuclear accumulation of mCAR was also observed with the hinge and LBD fragments. Since mutation or deletion of the hinge NLS did not completely block PB-induced nuclear accumulation, this sequence contributes to, but is not strictly required for nuclear translocation. Similarly, nuclear accumulation of a human CAR mutant with the DBD, hinge region and part of the LBD deleted was still observed leading to the conclusion that the hinge region and DBD are not required for CAR nuclear translocation (Sueyoshi et al., 2002). However, in the study of Sueyoshi et al., 2002, the nuclear levels of the truncated human CAR were not quantified so it is not clear if the nuclear accumulation was partially blocked as we observed with either the hinge or LBD fragments of mCAR. Interestingly, the decreased nuclear accumulation in PB-treated mice after mutation of the hinge NLS was largely reversed by fusion of the SV40 NLS to the mutant. This

DMD Fast Forward. Published on June 13, 2007 as DOI: 10.1124/dmd.107.016493
This article has not been copyedited and formatted. The final version may differ from this version.

result suggests that the hinge NLS is not directly activated by PB treatment, but that PB reverses a second signal in CAR that prevents nuclear translocation mediated by the hinge NLS.

An NES sequence has not been reported for CAR. Our previous observation of a modest increase in nuclear localization of the mCAR with Cys in the DBD mutated (Xia and Kemper, 2005) raised the possibility that the DBD might function as an NES for CAR, as it does for several other steroid and orphan nuclear receptors (Black et al., 2001). The DBDs of CAR and other nuclear receptors are highly conserved, including a di-Phe that is critical for NES function. Mutation of these Phe residues resulted in increased nuclear localization of full length mCAR or a mCAR fragment containing the DBD in hepatocytes *in vivo* in untreated mice. These results strongly indicate that the mCAR DBD contains an NES motif. The presence of an NES in mCAR in addition to the NLS's would be consistent with our proposal that CAR is a nucleocytoplasmic shuttling nuclear receptor (Xia and Kemper, 2005).

We were unable to demonstrate direct NES activity in the DBD using two assays in cultured Cos-1 cells (data not shown). In the first method (Black et al., 2001), the DBD was fused to a chimeric protein which included the glucocorticoid receptor LBD (GRLBD), and GFP. This chimera is cytoplasmic, but is translocated into the nucleus after dexamethoasone treatment unless the fused sequence contains an NES that competes with the ligand-activated NLS in the GRLBD. In the second method (Klemm et al., 1997), the putative mCAR NES was fused to the rapamycin binding domain of FRAP and coexpressed with a chimera containing a Gal4DBD, an NLS, and tandem repeats of the immunophilin, FKBP. Treatment with rapamycin would result in an interaction between the two chimeras and relocation of the FKBP-containing chimera to the cytoplasm if the mCAR sequence was an NES. In neither case was NES activity observed for the mCAR DBD. Since in both cases the NES activity must compete with an NLS, it is possible

that the mCAR sequence is a relatively weak NES that cannot efficiently compete with the NLS's in these assays.

The XRS motif was originally identified as a xenobiotic response signal since mutation of the XRS motif resulted in the loss of PB-induced nuclear accumulation of human CAR (Zelko et al., 2001), mCAR in hepatocytes *in vivo* (Xia and Kemper, 2005), and rat CAR in primary cultured hepatocytes (Kanno et al., 2005). Further, mutation of the XRS blocked nuclear translocation of CAR in untreated HepG2 cells and translocation mediated by exogenous expression of GRIP1 in hepatocytes *in vivo* (Xia and Kemper, 2005). These latter results suggested that the XRS motif was essential for nuclear import of mCAR independent of PB activation. Since mutation of the XRS blocks nuclear translocation, XRS probably functions as a positive signal for nuclear translocation that is masked in untreated animals rather than as a cytoplasmic retention signal. Supporting this conclusion, fusing an SV40 NLS sequence to the N-terminus of full length mCAR resulted in a modest increase in nuclear localization in untreated animals for both wild type and XRS mutant mCAR. However, additional PB-induced nuclear accumulation of the mutant mCAR with the fused NLS was still blocked so that the XRS is not acting just as an NLS activated by PB treatment. Some constructions containing the XRS, i.e hinge mutations and ΔCRR, are not PB responsive indicating that the XRS is not sufficient alone for PB-medicated nuclear translocation of mCAR. Further, a chimeric protein containing (1-116)mCAR and the LBD of PXR, (i.e., without the mCAR XRS) was present in the cytoplasm in hepatocytes *in vivo* and translocated to the nucleus similarly to wild type CAR after PB treatment (Hosseinpour et al., 2006). Therefore, the XRS is required for nuclear transport independent of PB treatment but is not sufficient or required, in the CAR/PXR chimera, for PB-mediated nuclear accumulation and, thus, is not likely a direct target of PB.

Cytoplasmic retention of CAR also contributes to the subcellular distribution of CAR. In untreated animals, CAR is retained in the cytoplasm as a complex with Hsp90 and CCRP (Kobayashi et al., 2003; Yoshinari et al., 2003). After PB treatment, protein phosphatase 2A is recruited to the complex and CAR is presumably released and translocated into the nucleus. CCRP was shown to interact with the LBD of CAR, but the motif was not identified. A cytoplasmic retention region (CRR) was identified in the LBD of rat CAR (Kanno et al., 2005) which is conserved in mCAR. Mutation or deletion of the CRR in rat CAR resulted in increased nuclear localization in untreated rat primary hepatocytes. Analogous mutations of mCAR, GFPCAR(1-220) and GFPCAR(ΔCRR), also exhibited increased nuclear localization in mouse hepatocytes *in vivo,* although the shift was not as dramatic as that observed with the rat CAR. These results are consistent with a cytoplasmic retention function within the region 220-258 and its location in the LBD is consistent with it functioning as a binding site for CCRP, but this has not been shown directly. Interestingly, deletion of the CRR does not result in nuclear accumulation equivalent to that observed after PB treatment. In addition to the reversal of cytoplasmic retention, therefore, PB must also actively mediate increased nuclear translocation.

The mechanism regulating the cellular localization of CAR, which is critical to the function of this constitutively active transcription factor, is clearly complex. In untreated animals, the NLS's and XRS must be either weak signals or masked since fusion of an SV40 NLS results in substantial nuclear accumulation. The PXR/CAR fusion study suggests that the PB responsive target is within the N-terminal 116 amino acids (Hosseinpour et al., 2006), but CAR with truncations in the C-terminus or mutation of the XRS which retain the first 116 amino acids are not PB responsive suggesting that there are C-terminal sequences which block the PB-mediated nuclear transport function of the N-terminal region. The CRR functions in untreated

animals, possibly by binding CCRP. A reasonable mechanism is that CCRP binding blocks the NLS and the XRS functions either directly or by altering the conformation of CAR. PB treatment results in a PP2A-mediated dephosphorylation that causes dissociation of CCRP and activation of the NLS and XRS functions. The recent demonstration of the importance of dephosphorylation of Ser-202 for nuclear accumulation, which is near the CRR, would be consistent with this mechanism (Hosseinpour et al., 2006). The XRS sequence resembles a protein-protein interaction motif so that an unknown protein that is necessary for nuclear translocation may bind to the XRS as has been suggested (Zelko et al., 2001). The NES may function to reduce nuclear concentrations in untreated animals or to export CAR after PB treatment to terminate the activation. The effect of PB treatment on the NES function is not known. To clearly resolve the role of these different motifs in CAR cellular localization, the proteins binding to each motif must be identified and the effects of PB treatment on the binding of the proteins and on posttranslational modification of CAR will need to be elucidated.

Acknowledgements

We thank Jeong-Ho Kim and Dr. Jie Chen for supplying plasmids for the cell-based nuclear export assays.

References

Baes M, Gulick T, Choi H-S, Grazia M, Martinoli G, Simha D and Moore DD (1994) A new orphan member of the nuclear hormone receptor superfamily that interacts with a subset of retinoic acid response elements. *Mol Cell Biol* **14:**1544-1552.

Black BE, Holaska JM, Rastinejad F and Paschal BM (2001) DNA binding domains in diverse nuclear receptors function as nuclear export signals. *Curr Biol* **11:**1749-1758.

Fischer U, Huber J, Boelens WC, Mattaj IW and Luhrmann R (1995) The HIV-1 Rev activation domain is a nuclear export signal that accesses an export pathway used by specific cellular RNAs. *Cell* **82:**475-483.

Hosseinpour F, Moore R, Negishi M and Sueyoshi T (2006) Serine 202 regulates the nuclear translocation of constitutive active/androstane receptor. *Mol Pharmacol* **69:**1095-1102.

Ikuta T, Eguchi H, Tachibana T, Yoneda Y and Kawajiri K (1998) Nuclear localization and export signals of the human aryl hydrocarbon receptor. *J Biol Chem* **273:**2895-2904.

Kaffman A and O'Shea EK (1999) Regulation of nuclear localization: a key to a door. *Annu Rev Cell Dev Biol* **15:**291-339.

Kanno Y, Suzuki M, Nakahama T and Inouye Y (2005) Characterization of nuclear localization signals and cytoplasmic retention region in the nuclear receptor CAR. *Biochim Biophys Acta* **1745:**215-222.

Kawata M (2001) Subcellular steroid/nuclear receptor dynamics. *Arch Histol Cytol* **64:**353-368.

Klemm JD, Beals CR and Crabtree GR (1997) Rapid targeting of nuclear proteins to the cytoplasm. *Curr Biol* **7:**638-644.

Kobayashi K, Sueyoshi T, Inoue K, Moore R and Negishi M (2003) Cytoplasmic accumulation of the nuclear receptor CAR by a tetratricopeptide repeat protein in HepG2 cells. *Mol Pharmacol* **64:**1069-1075.

Maruvada P, Baumann CT, Hager GL and Yen PM (2003) Dynamic shuttling and intranuclear mobility of nuclear hormone receptors. *J Biol Chem* **278:**12425-12432.

Min G, Kemper JK and Kemper B (2002) Glucocorticoid receptor interacting protein-1 (GRIP-1) and constitutive androstane receptor (CAR) mediate ligand-independent activation of the CYP2B1 gene in vivo. *J Biol Chem* **277:**26356-26363.

Moore LB, Parks DJ, Jones SA, Bledsoe RK, Consler TG, Stimmel JB, Goodwin B, Liddle C, Blanchard SG, Willson TM, Collins JL and Kliewer SA (2000) Orphan nuclear receptors constitutive androstane receptor and pregane X receptor share xenobiotic and steroid ligands. *J Biol Chem* **275:**15122-15127.

Sueyoshi T, Kawamoto T, Zelko I, Honkakoski P and Negishi M (1999) The repressed nuclear receptor CAR responds to phenobarbital in activating the human *CYP2B6* gene. *J Biol Chem* **274:**6043-6046.

Sueyoshi T, Moore R, Pascussi JM and Negishi M (2002) Direct expression of fluorescent protein-tagged nuclear receptor CAR in mouse liver. *Methods Enzymol* **357:**205-213.

Tzameli I, Pissios P, Schuetz EG and Moore DD (2000) The xenobiotic compound 1,4-bis[2-(3,5-dichloropyridyloxy)]benzene is an agonist ligand for the nuclear receptor CAR. *Mol Cell Biol* **20:**2951-2958.

Wen W, Meinkoth JL, Tsien RY and Taylor SS (1995) Identification of a signal for rapid export of proteins from the nucleus. *Cell* **82:**463-473.

Xia J and Kemper B (2005) Structural determinants of CAR required for its GRIP1-mediated nuclear accumulation. *J Biol Chem* **280:**7285-7293.

Yoshinari K, Kobayashi K, Moore R, Kawamoto T and Negishi M (2003) Identification of the nuclear receptor CAR:HSP90 complex in mouse liver and recruitment of protein phosphatase 2A in response to phenobarbital. *FEBS Lett* **548:**17-20.

Zelko I, Sueyoshi T, Kawamoto T, Moore R and Negishi M (2001) The peptide near the C terminus regulates receptor CAR nuclear translocation induced by xenochemicals in mouse liver. *Mol Cell Biol* **21:**2838-2846.

Footnotes

This work was supported by NIH Grant GM39360.

Person to receive reprint requests: Byron Kemper, Department of Molecular and Integrative Physiology, University of Illinois at Urbana-Champaign, 524 Burrill Hall, 407 S. Goodwin Ave. Urbana, IL 61801.

[1]Present address: Division of Oncology, Department of Medicine, Washington University, 660 S.Euclid Avenue, St. Louis, MO 63110

Figure Legends

Figure 1. Schematic diagrams of mCAR and truncated mCAR mutants. At the top, full length mCAR is shown with the locations of the DBD, Hinge, LBD and AF-2 domains indicated. The positions of the CRR, two Phe residues mutated in the DBD, and the sequences of the NLS in the hinge region (NLS1) and the XRS in the LBD, with residues mutated in these studies in underlined italics, are shown. Below full length mCAR, schematic diagrams of truncated mCAR mutants are shown. For localization studies, each of these constructs was fused to the C-terminus of GFP.

Figure 2. Representative images of hepatocytes expressing GFP-mCAR. Hepatocytes were transfected *in vivo* by injection of expression vector DNA for NLSL322A/326A/329A into the tail vein of mice. Cells from untreated mice were imaged by confocal microscopy as described in "Materials and Methods". An image of a representative cell in each of the four RNF categories, <0.25 (A), 0.25-0.5 (B), 0.5-0.75 (C), and >0.75 (D) is shown. Both red and green fluorescence is shown on the left for each cell and only green fluorescence is shown on the right. Red fluorescence is from propridium iodide staining of DNA and marks the nucleus and green is fluorescence from the GFP-mCAR chimera. Additional representative images of cells have been shown previously (Min et al., 2002; Xia and Kemper, 2005).

Figure 3. Analysis of mCAR sequences involved in cytoplasmic to nuclear translocation. To transfect hepatocytes *in vivo*, expression vector DNA for GFP chimeras of mCAR or mutant mCARs was injected into the tail veins of mice. Schematic diagrams of the truncated constructions are illustrated in Fig. 1. Mice were treated with saline or PB 2 hr after injection of DNA as indicated and were sacrificed 6 hr later. Forty to 100 cells were randomly selected for each mCAR construction from confocal images of liver sections and the GFP fluorescence

intensity in the nucleus (In) and the cytoplasm (Ic) was quantified as described in "Materials and Methods". The mean and standard error of the values for RNF are shown in the panels. ** $p < 0.01$ for the mutant compared to the corresponding wild type and †† $p < 0.01$ for the untreated (C) samples compared to PB-treated (P) samples as determined by the Student's t-test, n = 40 to 100. A. The cellular distribution of full length wild type (WT) mCAR (a), mCAR fragments that contained the hinge domain (b) or the LBD (c) was analyzed. B. The cellular distribution was determined of CAR with substitutions of Ala for Leu at positions 322, 326, and 329 in the XRS (L322/6/8A) (a) and of wild type mCAR (b) or the XRS mutant (c) with the SV40 NLS fused at the N-terminus. C. The cellular distribution was determined for mCAR with substitutions of Ala for Arg at either positions 107 and 108 (R107/8A, a) or at 107, 108, 114, and 115 (4RA, b) in the proposed hinge domain NLS or for the R107A/R108A mutant with the SV40 NLS fused at the N-terminus (NLSR107/8A, c). D. The cellular distribution was determined for the mCAR fragment from 1-220 (a) which deletes both the CRR and the XRS sequences, or for mCAR with the CRR sequence from 220 to 258 deleted (b). Data for wild type mCAR (WT) and the mutant L322/L326A/L329A are from Xia and Kemper (Xia and Kemper, 2005).

Figure 4. Analysis of mCAR sequences involved in nuclear to cytoplasmic translocation. Hepatocytes were transfected *in vivo* with expression vector DNA of GFP chimeras of mCAR or mutant mCARs and cellular distribution of fluorescence was determined in livers of PB-treated mice as described in the legend to Fig. 3. The cellular distribution was determined for full length mCAR, either wild type (WT) (A) or with Ala substituted for Phe 44 and Phe 45 (F44/5A) (B), or for a mCAR fragment containing the DBD, either wild type (DBD) (C) or with the two Phe residues mutated (DBDF44/5A) (D). The mean and standard error of the values for relative

nuclear fluorescence are shown in the panels. ** $p < 0.01$ for the mutants compared to the corresponding wild types or the mCAR DBD compared with full length mCAR as determined by the Student's t-test, n = 40 to 80.

Figure 1

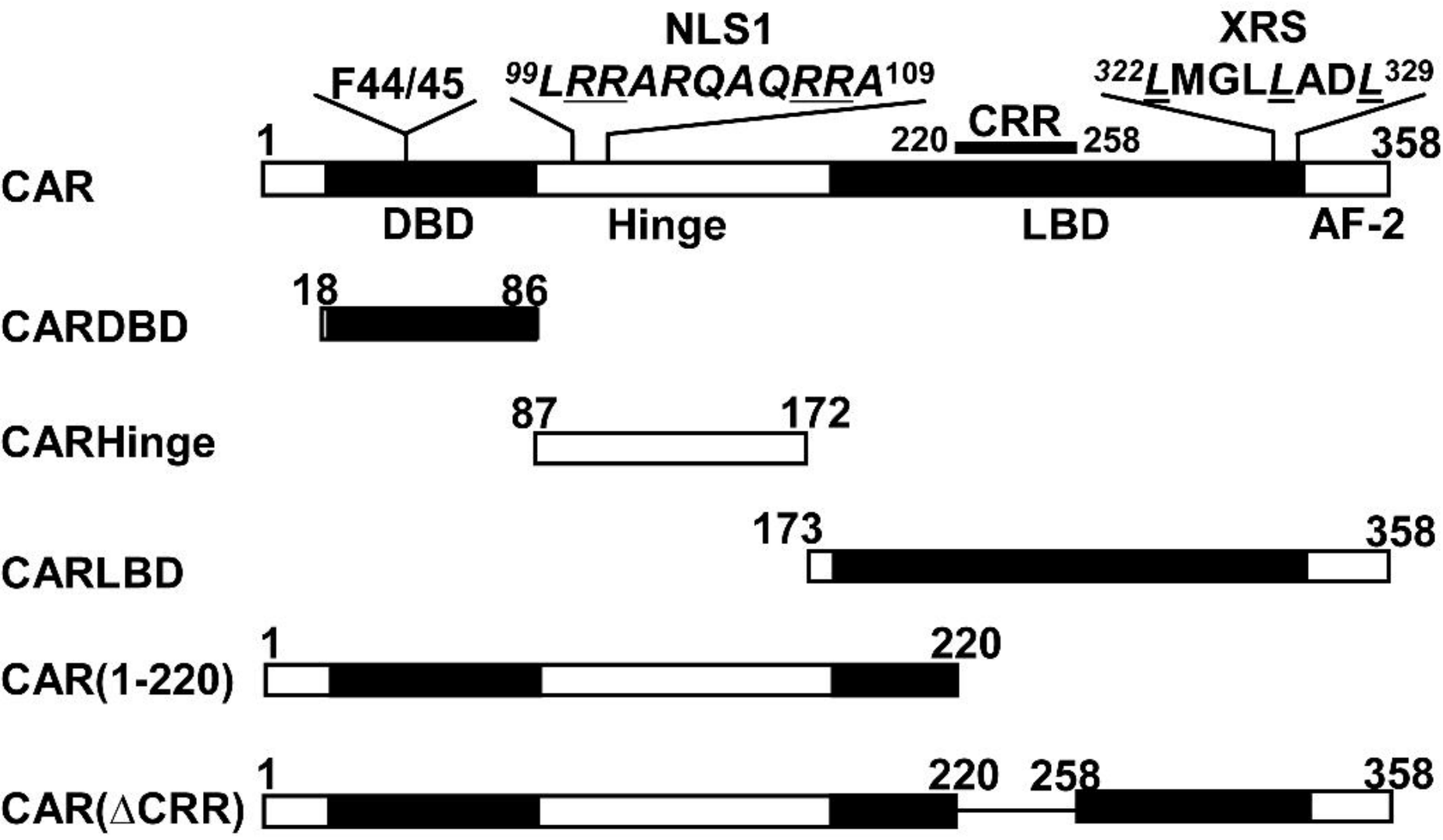
NLS1
XRS
F44/45
99LRRARQAQRRA109
322LMGLLADL329
CRR
1
220
258
358
CAR
DBD
Hinge
LBD
AF-2
18
86
CARDBD
87
172
CARHinge
173
358
CARLBD
1
220
CAR(1-220)
1
220
258
358
CAR(ΔCRR)

Figure 2

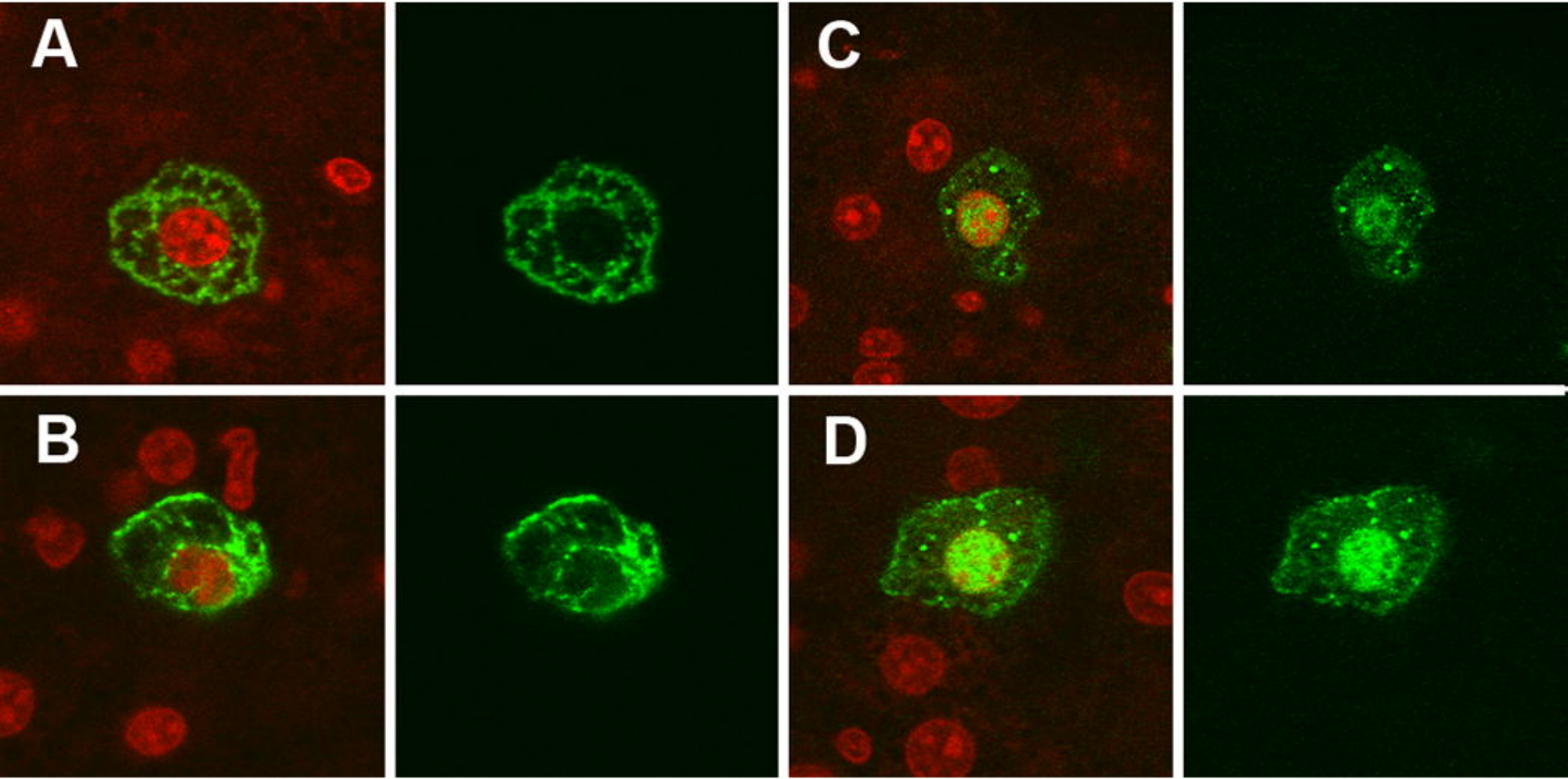

Figure 3

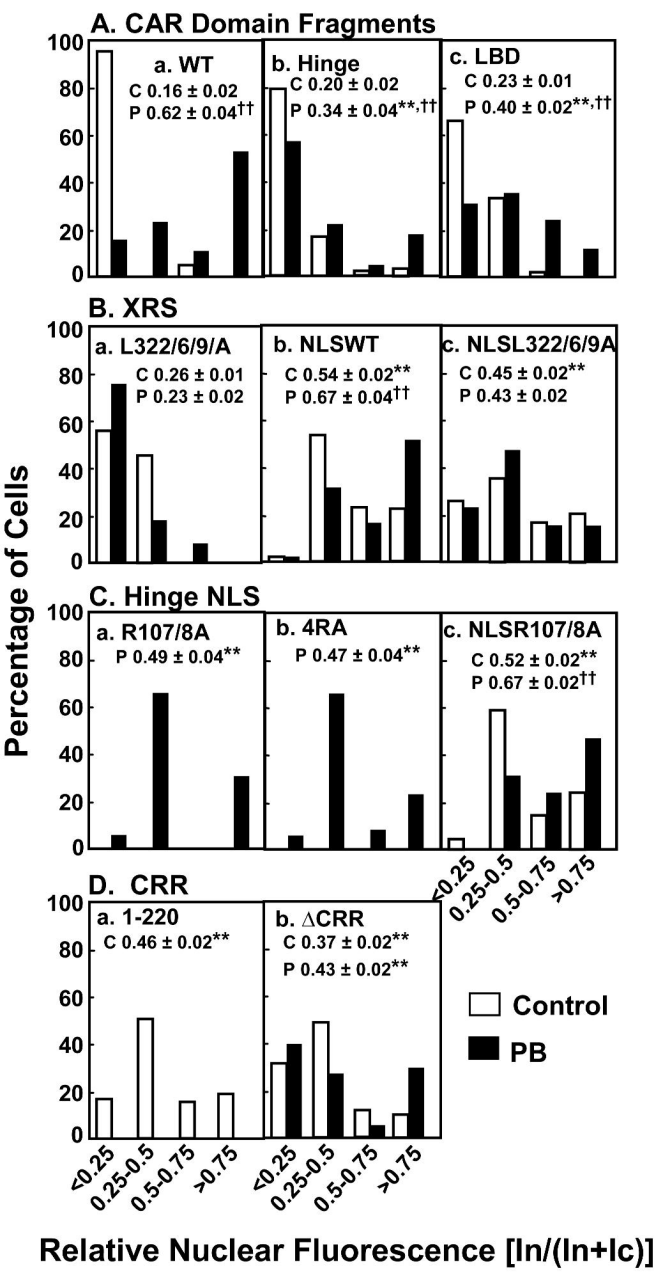
A. CAR Domain Fragments
a. WT
C 0.16 ± 0.02
P 0.62 ± 0.04††
b. Hinge
C 0.20 ± 0.02
P 0.34 ± 0.04**,††
c. LBD
C 0.23 ± 0.01
P 0.40 ± 0.02**,††
B. XRS
a. L322/6/9/A
C 0.26 ± 0.01
P 0.23 ± 0.02
b. NLSWT
C 0.54 ± 0.02**
P 0.67 ± 0.04††
c. NLSL322/6/9A
C 0.45 ± 0.02**
P 0.43 ± 0.02
C. Hinge NLS
a. R107/8A
P 0.49 ± 0.04**
b. 4RA
P 0.47 ± 0.04**
c. NLSR107/8A
C 0.52 ± 0.02**
P 0.67 ± 0.02††
D. CRR
a. 1-220
C 0.46 ± 0.02**
b. ΔCRR
C 0.37 ± 0.02**
P 0.43 ± 0.02**
Percentage of Cells
0
20
40
60
80
100
<0.25
0.25-0.5
0.5-0.75
>0.75
Control
PB
Relative Nuclear Fluorescence [In/(In+Ic)]

Figure 4

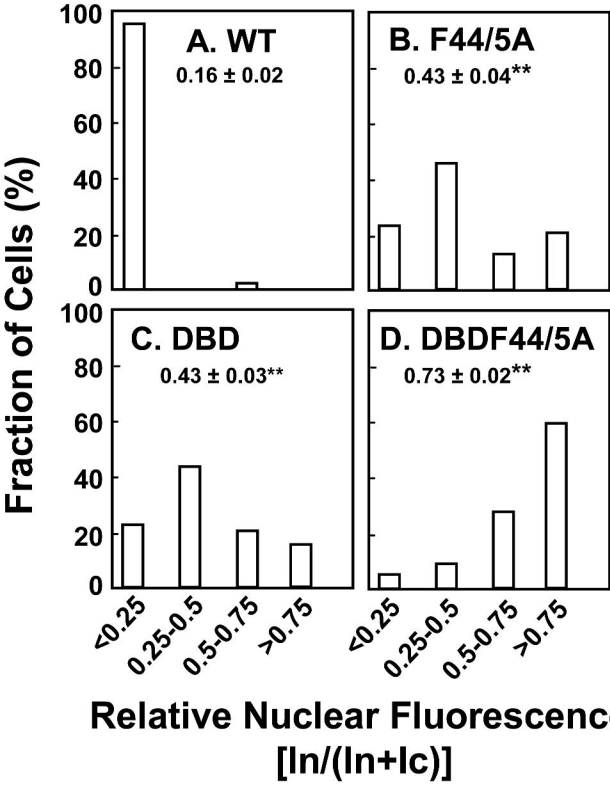
A. WT
0.16 ± 0.02
B. F44/5A
0.43 ± 0.04**
C. DBD
0.43 ± 0.03**
D. DBDF44/5A
0.73 ± 0.02**
Fraction of Cells (%)
100
80
60
40
20
0
<0.25
0.25-0.5
0.5-0.75
>0.75
Relative Nuclear Fluorescence
[In/(In+Ic)]